Journal of Mathematics and Computing Science, 11 (2): 96-109, 2025

eISSN: 0128-0767

Bifurcation Analysis of Stage-structured Prey-predator Interactions in Sea Turtle Populations

Zati Iwani Abdul Manaf[1*], Muhammad Arif Azhar Khairulriza[2], Muhammad Syauqi Abdul Ghani[3] and Nur Syasya Iwanie Mohd Arifin[4]

[1,2,3,4]Faculty of Computer and Mathematical Sciences, Universiti Teknologi MARA Kelantan, Bukit Ilmu, Machang, Kelantan, Malaysia

Authors' email: zati431@uitm.edu.my*, muhammadarifazhar2002@gmail.com, syauqighani8@gmail.com and syasyaiwanie02@gmail.com

*Corresponding author

Received **; Received in revised **; Accepted ***
Available online ***
DOI: https://doi.org/10.24191/jmcs.*******

Abstract: In this study, a stage-structured prey-predator model is used to describe the dynamics of sea turtles and their marine predators across different life stages. Marine predators primarily target hatchlings, while mature sea turtles can survive independently and immature individuals often rely on external support. This paper employs stability analysis and bifurcation analysis and treating the conversion rate from sea turtle eggs to hatchlings as the bifurcation parameter. Graphical results, including bifurcation diagrams, phase-plane plots, and time series graphs, are produced with XPPAUT, Maple, and MATLAB, respectively. The analysis identifies a transcritical bifurcation point that marks a change in system stability under varying conversion rates. Moreover, the results demonstrate that the conversion rate strongly influences prey-predator dynamics: low rates can cause predator extinction, moderate rates allow coexistence, and high rates increase predation on hatchlings. Overall, the study highlights the ecological importance of hatching rates for maintaining balance and guiding conservation strategies, with particular attention to preventing species extinction.

Keywords: Bifurcation analysis, Lotka-Volterra model, Sea turtles, Transcritical bifurcation, Numerical simulation

1 Introduction

Prey-predator interaction describes the relationship between two organisms in which one species relies on the other as a food source [1], [2], [3]. Through predation, energy is transferred between organisms and across trophic levels. Predators often share certain traits: they are usually larger than their prey and frequently target young or vulnerable individuals [4], [5], [6]. It is also common for a species to function as both prey and predator, depending on its position in the food web. In ecological systems, food chains depict how energy moves from producers to consumers and decomposers [7], [8]. When these chains are interconnected, they form a food web that reflects the interdependence of many trophic groups within an ecosystem [9].

Sea turtles provide a useful example for studying prey-predator dynamics because they are endangered and face numerous natural threats [10]. Their reproductive pattern follows a K-strategy: females lay relatively few clutches, each containing roughly 65 to 180 eggs [11]. Their slow growth

and long lifespan, which is around 75 to 100 years, mean that sexual maturity is only reached at about 20 to 30 years of age. Sea turtles also exhibit natal homing, returning to their birthplace to nest after long migrations guided by geomagnetic cues [12], [13]. Although this behaviour helps turtles return to suitable nesting sites, it also increases their exposure to changing environmental conditions. Turtle eggs receive almost no parental protection, and nests are placed in different types of locations, which can influence incubation, hatching success, and early survival [14]. Common predators such as ghost crabs and black-tipped sharks feed on eggs, hatchlings, and young turtles on land and in the sea [10]. As turtles grow larger, they become less vulnerable to these predators, and the risk of predation decreases sharply [15].

Recent studies have examined the stability of prey-predator systems involving sea turtles and human activities [16], [17], [18]. These studies show how harvesting, egg collection, and environmental disturbance can affect long-term population trends. Researchers have also used stage-structured prey–predator models to improve on the classical Lotka-Volterra approach [19]. These models divide a population into key life stages (e.g., eggs, hatchlings, juveniles, and adults) so that age-specific survival and reproduction can be modelled more realistically.

Several extensions of stage-structured prey-predator models have been explored. For example, Roslan et al. [16] studied human egg consumption and found that heavy harvesting greatly reduces the probability of sea turtle population survival. In a related study, Khairuddin et al. [17] included nest exploitation and showed that predation and harvesting can either collapse or maintain turtle populations, depending on the conditions. In another direction, Lutfi et al. [18] introduced a discrete-time model to predict whether populations will coexist or go extinct under different levels of exploitation. Their results showed that such model can capture generational shifts, especially when human activity is a factor. Meanwhile, Dubey and Kumar [19] added time delays to a stage-structured model and found that growth or reproductive delays can create complex population patterns. Their study showed that even small delays can strongly influence system behaviour.

More recent studies also show how early-life stages and bifurcation patterns can shape population outcomes. Herrera et al. [20] found that small changes in egg or hatchling survival can shift sea turtle populations between persistence and decline. Their work highlights the importance of modelling early-life transitions accurately. Aguilera et al. [21] further advanced prey-predator theory by showing that nonlinearities in stage-transition terms may reveal hidden bifurcation behaviour not detectable in unstructured models. These underscores the need for detailed life-history representation. In addition, Roslan et al. [22] examined the influence of coastal pollution on turtle-predator interactions and found that environmental contaminants can alter stability outcomes by affecting hatchling survival and predator responses. In a related study, Roslan et al. [23] further employed bifurcation analysis to identify ecological thresholds associated with marine debris impacts, demonstrating how small environmental changes may separate extinction regimes from coexistence regions. Most recently, Siaw et al. [24] analysed a stage-structured turtle-predator system with variable early-life processes and showed that conversion rates between stages strongly affect whether prey and predators persist. Overall, these studies highlight that early-life transitions, especially the conversion of eggs to hatchlings, play a major role in shaping prey-predator dynamics.

Building on the earlier study, Khairuddin et al. [10] developed a stage-structured prey-predator model for green turtles at Chagar Hutang Beach, Malaysia. Their findings showed that the system can lead to either extinction or coexistence depending on parameter values. Although their study provided valuable ecological insight, it did not examine how small changes in life-stage conversion influence system stability. This gap raises the question of how hatching success affects system behaviour and predator persistence. To address this, the present study extends the analysis in [10] by applying stability and bifurcation techniques, focusing on the conversion rate as the bifurcation parameter. This approach offers a clearer understanding of early-life sensitivity and provides information to guide conservation efforts.

2 Methods

This section presents the formulation of the stage-structured prey-predator model, the determination of equilibrium points, the stability analysis, and the numerical simulations. Figure 1 illustrates the methodological framework adopted in this study.

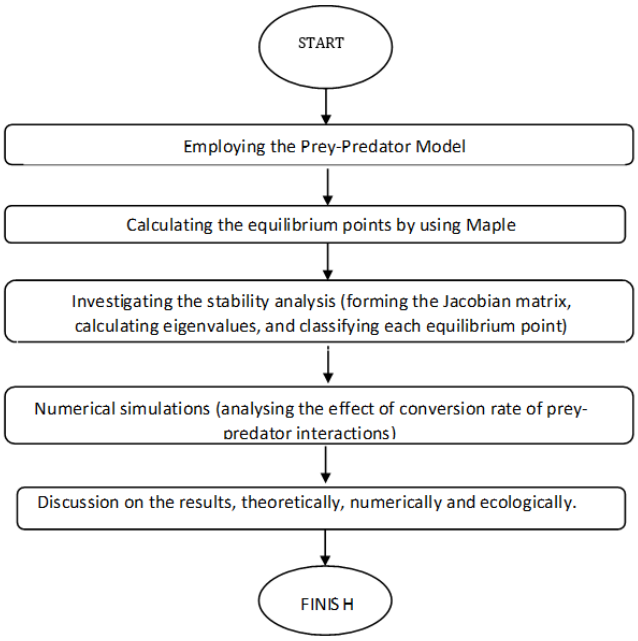

Figure 1: The flow diagram of the research method

A The Lotka-Volterra Model

This study considers a two-species system that incorporates both mature and immature prey, together with a predator population. The system extends the work of Khairuddin et al. [10], by analysing the effects of the conversion rate on prey-predator interactions. Hence, the Lotka-Volterra system is written as:

$$\begin{aligned} \frac{dx}{dt} &= rx(1-\frac{x}{k}) - ax - wx, \\ \frac{dy}{dt} &= gwx - cy - byz, \\ \frac{dz}{dt} &= fbyz - sz. \end{aligned} \tag{1}$$

Here, x represents sea turtle eggs, y denotes hatchlings, and z is the marine predator population. Each equation reflects the main biological processes affecting the three stages. Each equation reflects the main biological processes affecting the three stages. The term $rx\left(1-\frac{x}{k}\right)$ models egg production, where r is the egg deposition rate and the logistic factor accounts for limited nesting space represented by the carrying capacity, k. Eggs are also reduced by natural losses (ax) and by hatching (wx), which moves individuals into the hatchling stage. Hatchlings increase when eggs hatch successfully (gwx), and decline due to non-predatory causes (cy) as well as predation (byz), which depends on encounters

between predators and hatchlings. The predator population grows when hatchlings are consumed $(fbyz)$, and decreases through natural mortality (sz). Together, these terms capture the basic flow of the sea turtles across life stages and the key ecological interactions that shape their dynamics.

Two biological assumptions are made in system (1). First, the carrying capacity, k, is assumed as constant. This reflects the fact that the amount of nesting space on a beach does not change much from one season to another unless major environmental events occur. Second, density-dependent effects among hatchlings are ignored. This is reasonable because hatchlings spread out quickly after reaching the sea, and their survival is influenced far more by predators and environmental conditions than by competition among themselves. Such assumptions are commonly used in models of sea turtle populations [10], [17], [18], [19]. Thus, all variables and parameters are summarised in Table 1.

Table 1 : Summary of variables and parameters used in system (1)

Symbol	Description
$x(t)$	Number of sea turtle eggs laid in nests
$y(t)$	Number of newly hatched juveniles entering the sea
$z(t)$	Marine predator population feeding on hatchlings
r	Egg deposition rate per adult turtle
k	Carrying capacity (maximum egg capacity of the nesting beach)
a	Natural egg mortality rate (loss of eggs due to non-predatory factors)
w	Hatching rate (the fraction of eggs that hatch successfully)
g	Egg-to-hatchling conversion rate (the success of hatchlings reaching the water)
c	Natural hatchling mortality (non-predatory losses during early movement to the sea)
b	Predation rate (how often predators capture hatchlings)
s	Natural predator mortality rate (predator loss in the absence of prey)
f	Conversion efficiency (how effectively predators gain growth from consuming hatchlings)

With all variables and parameters clearly defined, the mathematical properties of system (1) can now be examined to ensure that the model produces biologically meaningful solutions.

B Positivity

The positivity of solutions is an essential requirement for biological models, as negative population values have no ecological meaning. Before presenting the formal result, it is useful to outline the structure of the proof. The positivity analysis is carried out in the order x, z, and then y. This ordering is chosen because the differential equations for x and z are independent of y, which allows their positivity to be established first. Once the behaviour of $x(t)$ and $z(t)$ is confirmed, the positivity of $y(t)$ follows naturally from the form of its linear equation. This sequence clarifies the logical flow of the argument and reflects the dependence of each variable in system (1). The following theorem establishes the positivity of solutions to system (1):

Theorem 1. *Let* $r,k,a,w,g,c,b,f,c>0$. *For any initial conditions* $x(0)\geq 0, y(0)\geq 0, z(0)>0$, *the solution of system (1) satisfy* $x(t)\geq 0, y(t)\geq 0, z(t)>0$ *for all* $t\geq 0$. *If the initial conditions are strictly positive, then* $x(t), y(t), z(t)>0$ *for all* $t\geq 0$.

Proof. On any subinterval where a component is positive, division by that component is valid, and integration yields closed-form expressions:

i) For x:

$$\frac{1}{x}\frac{dx}{dt} = r\left(1-\frac{x}{k}\right) - a - w \quad \Rightarrow \quad x(t) = x(0)e^{\int_0^t \left[r\left(1-\frac{x(\theta)}{k}\right)-a-w\right]d\theta} \geq 0.$$

If $x(0) = 0$, then $\left.\frac{dx}{dt}\right|_{t=0} = 0$ and by uniqueness, $x(t) \equiv 0$.

ii) For z:

$$\frac{1}{z}\frac{dz}{dt} = fby - s \quad \Rightarrow \quad z(t) = z(0)e^{\int_0^t [fby(\theta)-s]d\theta} \geq 0.$$

If $z(0) = 0$, then $\left.\frac{dz}{dt}\right|_{t=0} = 0$ and hence $z(t) \equiv 0$.

iii) For y: the equation $\frac{dy}{dt} + (c + bz(t))y = gwx(t)$ is linear. With integrating factor,

$$\mu(t) = e^{\int_0^t (c+bz(\theta))d\theta} > 0,$$

$$y(t) = y(0)e^{-\int_0^t (c+bz(\theta))d\theta} + \int_0^t e^{-\int_0^t (c+bz(\tau))d\tau} gwx(s)ds \geq 0.$$

All exponentials are non-negative and the source term gwx is non-negative. Therefore $x(t) \geq 0, y(t) \geq 0, z(t) > 0$ for all $t \geq 0$. If the initial conditions are strictly positive, each expression above is strictly positive for $t > 0$, which establishes strict positivity. Hence the proof.

C Stability Analysis

Stability analysis examines the dynamical behaviour of the system near equilibrium points. Setting the right-hand sides of system (1) to zero yields three equilibria:

$$E_1 = (0,0,0),$$

$$E_2 = \left(\frac{k(r-a-w)}{r}, \frac{gwk(r-a-w)}{cr}, 0\right),$$

$$E_3 = \left(\frac{k(r-a-w)}{r}, \frac{s}{fb}, \frac{fgwbk(r-a-w)}{rs} - \frac{c}{b}\right).$$

The Jacobian matrix of system (1) is:

$$J(x,y,z)=\begin{bmatrix} r\left(1-\frac{x}{k}\right)-\frac{rx}{k}-a-w & 0 & 0 \\ gw & -bz-c & -by \\ 0 & bfz & fby-s \end{bmatrix}. \quad (2)$$

Local stability is determined by the signs of the eigenvalues of J at each equilibrium. An equilibrium is locally asymptotically stable if all eigenvalues have negative real parts; otherwise, it is unstable (saddle). The detailed stability conditions are presented through Theorems 2-4, supported by explicit eigenvalue calculations and the Routh-Hurwitz criterion [25].

Theorem 2. *The trivial equilibrium* $E_1(0,0,0)$ *is locally asymptotically stable if* $r<a+w$*, and it is a saddle point if* $r>a+w$.

Proof. The stability of trivial equilibrium E_1 is examined by evaluating the eigenvalues of the Jacobian matrix (2) at E_1. Substituting $E_1(0,0,0)$ into (2) yields:

$$J(0,0,0)=\begin{bmatrix} r-a-w & 0 & 0 \\ gw & -c & 0 \\ 0 & 0 & -s \end{bmatrix}.$$

This triangular matrix has eigenvalues $\lambda_1=r-a-w$, $\lambda_2=-c$, and $\lambda_3=-s$. Since $c,s>0$, and $\lambda_2,\lambda_3<0$. Thus:

- if $r<a+w$, then $\lambda_1<0$ and all three eigenvalues are negative. Hence, E_1 is locally asymptotically stable.
- if $r>a+w$, then $\lambda_1>0$. Hence, E_1 has one positive eigenvalue and is a saddle.

This completes the proof.

Theorem 3. *The equilibrium* $E_2\left(\frac{k(r-a-w)}{r},\frac{gwk(r-a-w)}{cr},0\right)$ *is locally asymptotically stable if* $r>a+w$ *and* $g<\frac{crs}{kwbf(r-a-w)}$.

Proof. At E_2, the Jacobian (2) becomes:

$$J(E_2)=\begin{bmatrix} -(r-a-w) & 0 & 0 \\ gw & -c & -\dfrac{bgwk(r-a-w)}{cr} \\ 0 & 0 & \dfrac{fbgwk(r-a-w)}{cr}-s \end{bmatrix}.$$

Hence, the corresponding eigenvalues are:

$$\lambda_1=-(r-a-w), \qquad \lambda_2=-c, \qquad \lambda_3=\frac{fbgwk(r-a-w)}{cr}-s.$$

Local asymptotic stability requires all three eigenvalues to be negative. Clearly, $\lambda_2<0$. The inequility $\lambda_1<0$ holds iff $r>a+w$. Finally,

$$\lambda_3<0 \Leftrightarrow \frac{fbgwk(r-a-w)}{cr}-s<0 \Leftrightarrow g<\frac{crs}{kwbf(r-a-w)}.$$

Under these two inequalities, E_2 is is locally asymptotically stable. Hence the proof.

Theorem 4. *The interioir equilibrium point* $E_3(x^*,y^*,z^*)=\left(\dfrac{k(r-a-w)}{r},\dfrac{s}{fb},\dfrac{fgwbk(r-a-w)}{rs}-\dfrac{c}{b}\right)$ *is locally asymptotically stable if* $r>a+w$, $z^*>0$, and the Routh-Hurwitz conditions are satisfied. Equivalently, stability requires $g>\dfrac{crs}{fwk(r-a-w)}$.

Proof. At E_3, $x=x^*=\dfrac{k(r-a-w)}{r}$ and $y=y^*=\dfrac{s}{fb}$, so $fby^*-s=0$ and:

$$J\left(E_3\right)=\begin{bmatrix} -(r-a-w) & 0 & 0 \\ gw & -c-bz^* & -by^* \\ 0 & fbz^* & 0 \end{bmatrix}.$$

Hence, the characteristic polynomial of $J(E_3)$ is $\chi(\lambda)=\lambda^3+a_1\lambda^2+a_2\lambda+a_3$, with coefficients:

$$a_1=r-a-w+c+bz^*, \quad a_2=(r-a-w)(c+bz^*)+fb^2y^*z^*, \quad a_3=(r-a-w)fb^2y^*z^*.$$

For a cubic polynomial, the Routh-Hurwitz conditions for all roots to have negative real parts are:

$$a_1>0, \qquad a_2>0, \qquad a_3>0, \qquad a_1a_2>a_3.$$

Because $y^*=\dfrac{s}{fb}>0$, the inequalities $a_3>0$ holds whenever $r-a-w>0$ and $z^*>0$. Under these two conditions, $a_1>0$ is immediately, and $a_2>0$ follows from the positivity of each term. Moreover,

$$a_1a_2-a_3=(c+bz^*)\left[(r-a-w)^2+(r-a-w)(c+bz^*)+fb^2y^*z^*\right]>0,$$

since every factor is strictly positive. Thus, all Routh-Hurwitz conditions are satisfied. Therefore, E_3 is locally asymptotically stable provided $r-a-w>0$ and $z^*>0$. The condition $z^*>0$ is equivalent to:

$$fgwk(r-a-w)-crs>0 \qquad \Leftrightarrow \qquad g>\frac{crs}{fwk(r-a-w)}.$$

This completes the proof.

3 Results and Discussion

The analysis of system (1) is carried out using the parameter values listed in Table 2. These values are selected based on ecological studies of sea turtles and related modelling literature, with some parameters assumed in order to facilitate numerical simulations. In particular, the parameters r, a, w and c are assumed and varied within reasonable ranges as part of the parameter variation technique implemented in XPPAUT [26], [27]. This technique allows the detection of bifurcation points by systematically varying parameters across the desired range. Among all parameters, the conversion rate g, representing the rate at which sea turtle eggs develop into hatchlings, is chosen as the bifurcation parameter. In this study, the parameter g is varied within the narrow interval $0.0067875<g<0.0067885$ to identify the bifurcation point and examine how small changes in hatching success influence system behaviour. Its ecological significance lies in the fact that small changes in hatching success can drastically influence predator survival and overall prey-predator dynamics. By applying one-parameter bifurcation analysis, the model captures how changes in g affect system stability and population persistence.

Table 2 : The parameter values used in system (1)

Parameters	Values	Sources
r	1.4	Assumed
k	700	[28]
a	0.6	Assumed
w	0.55	Assumed
c	0.01	Assumed
b	0.015	[29]
g	[0.0067875, 0.0067885]	Varied
s	0.7	[10]
f	1	[10]

A One-Parameter Bifurcation Analysis

One-parameter bifurcation analysis is a numerical technique used to investigate how the stability of equilibria changes as a single parameter is varied. In this study, the conversion rate g is selected as the bifurcation parameter to explore how hatching success influences prey-predator interactions. Using XPPAUT, the system exhibits a transcritical bifurcation, where the stability of equilibria is exchanged between predator extinction and predator persistence states. The corresponding bifurcation diagram is shown in Figure 2. In the diagram, the red curve represents stable equilibria, the black curve represents unstable equilibria, and the dashed blue line indicates the slicing of the bifurcation parameter. The point B marks the transcritical bifurcation, where stability exchanges between equilibria.

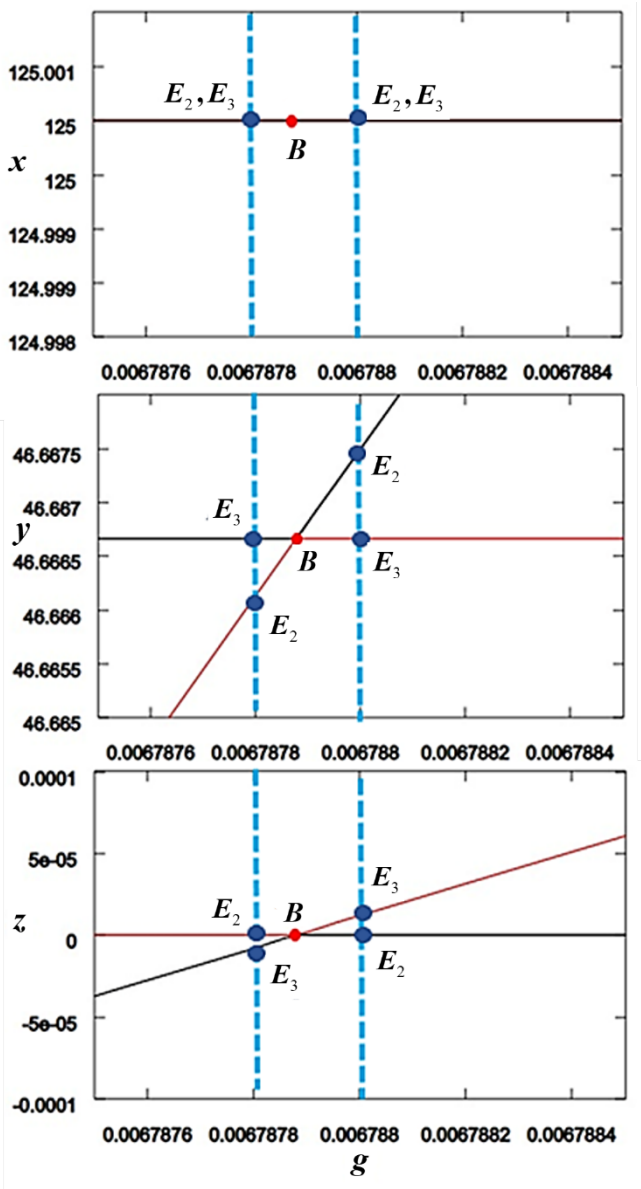

Figure 2: One-parameter bifurcation diagram for x, y and z plotted against the conversion rate g. The top panel shows the egg population, x, which remains almost constant across the tested range of, g, reflecting the stability of nesting capacity. The middle panel displays the hatchling population, y, where the transition from the unstable (black curve) to stable (red curve) equilibrium, E_3, illustrating how hatching success influences juvenile abundance. The bottom panel shows the marine predator population, z, which shifts from non-feasible values to positive stable values as g increases past the bifurcation point, B, indicating the ecological threshold required for predator persistence.

To demonstrate this switching of stability, the bifurcation diagram is sliced immediately before (e.g., $g = 0.0067878$) and after (e.g., $g = 0.006788$) the transcritical bifurcation point, B. At the lower slice, the equilibrium $E_2(125, 46.67, 0)$ is observed as an asymptotically stable node, while $E_3(125, 46.67, -0.000007)$ corresponds to a saddle. This behaviour is consistent with Theorem 3, which establishes the stability of E_2 under appropriate parameter conditions, and with Theorem 4, which shows that E_3 cannot be stable when the predator density is not biologically feasible. Although the predator density at this value of E_3 is slightly negative and thus not biologically unrealistic, the point

is retained in the analysis because it clearly demonstrates the switching of stability between equilibria at the bifurcation. Such outcomes are typical in bifurcation theory, where equilibrium branches may temporarily extend outside the biologically feasible region but remain essential for identifying stability exchanges [30].

In addition to this qualitative description, the analytical stability conditions in Theorems 3 and 4 can be viewed as a diagnosis across the parameter space of the conversion rate g. These conditions separate the model behaviour into two biologically meaningful regions. For values of g below the critical threshold at the bifurcation point, B, the predator population becomes extinct while the egg and hatchling populations persist at equilibrium. For g values above this threshold, the interior equilibrium becomes stable, and all three populations coexist. This provides a clear stability map in the parameter space of g, identifying the ranges that lead to predator extinction or prey-predator coexistence, and aligns with the behaviour illustrated in the bifurcation diagram.

When the bifurcation parameter increases slightly to $g = 0.006788$, the stability of the equilibria is reversed. The equilibrium $E_2(125, 46.67, 0)$ loses stability and becomes a saddle point, while $E_3(125, 46.67, 0.00001)$ shifts into the biologically feasible region and emerges as an asymptotically stable node. This transition confirms the prediction of Theorem 4, which demonstrates that the interior equilibrium E_3 is locally asymptotically stable whenever the predator population satisfies $z^* > 0$. At the same time, the instability of E_2 beyond this threshold is fully consistent with Theorem 3, since its stability condition is no longer satisfied. The trivial equilibrium $E_1(0,0,0)$ remains an unstable saddle throughout, in agreement with Theorem 2. The eigenvalues and stability classifications for these parameter slices are summarised in Table 3, which provides numerical evidence supporting the theoretical analysis.

Table 3: The stability analysis results

Critical Points	**Eigenvalues**	**Stability Results**
Conversion rate, $g = 0.0067878$		
$E_1 = (0,0,0)$	$\lambda_1 = 0.25, \lambda_2 = -0.01, \lambda_3 = -0.7$	Saddle
$E_2 = (125, 46.67, 0)$	$\lambda_1 = -0.25, \lambda_2 = -0.000008, \lambda_3 = -0.01$	Asymptotically stable node
$E_3 = (125, 46.67, -0.000007)$	$\lambda_1 = -0.25, \lambda_2 = 0.000008, \lambda_3 = -0.010008$	Saddle
Conversion rate, $g = 0.006788$		
$E_1 = (0,0,0)$	$\lambda_1 = 0.25, \lambda_2 = -0.01, \lambda_3 = -0.7$	Saddle
$E_2 = (125, 46.67, 0)$	$\lambda_1 = -0.25, \lambda_2 = 0.0000125, \lambda_3 = -0.01$	Saddle
$E_3 = (125, 46.67, 0.00001)$	$\lambda_1 = -0.25, \lambda_2 = -0.00001, \lambda_3 = -0.00999$	Asymptotically stable node

The phase planes are further plotted using MATLAB to visualise the population trajectories for these conversion rate values. Five different initial conditions are represented by coloured curves in Figure 3, which depicts the phase portraits at the equilibria $E_2 = (125, 46.67, 0)$ and $E_3 = (125, 46.67, 0.00001)$. At the lower conversion rate (e.g., $g = 0.0067878$), trajectories converge towards E_2 confirming its role as an asymptotically stable node where eggs and hatchlings persist while predators go extinct. Meanwhile, at the higher conversion rate (e.g., $g = 0.006788$), trajectories instead converge towards E_3, which becomes biologically feasible and asymptotically stable. The phase plane at E_3 illustrates that once the conversion rate of newly hatched juveniles exceeds the threshold, all populations coexist in a stable state. These results, together with the bifurcation diagram in Figure 2 and the stability conditions in Theorems 2-4, provide strong numerical confirmation of the theoretical predictions.

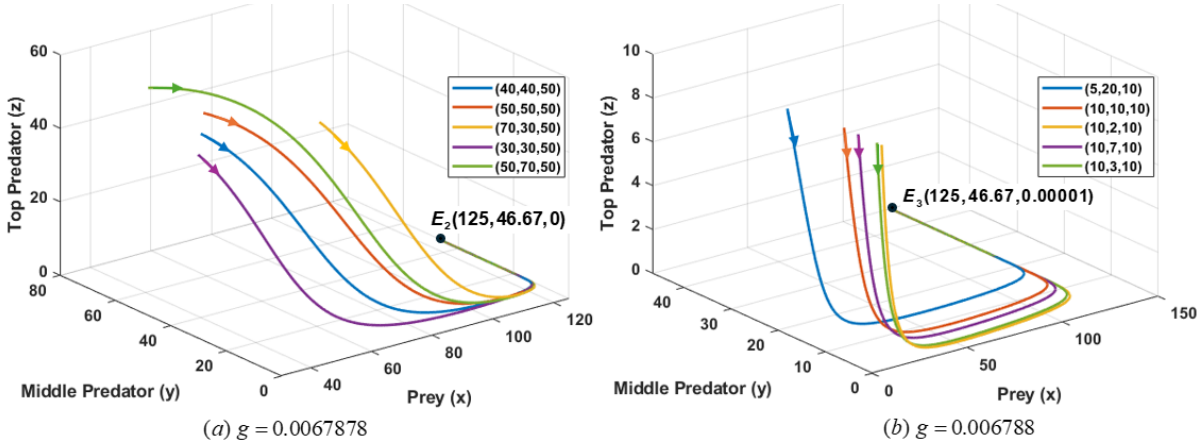

(*a*) $g = 0.0067878$ (*b*) $g = 0.006788$

Figure 3: 3D phase portrait of system (1) at the equilibria E_2 for $g = 0.0067878$ and E_3 for $g = 0.006788$. Coloured curves represent trajectories from different initial conditions

B Dynamical Behaviour of Species under Varying Conversion Rates

To further illustrate the system dynamics, time series simulations are performed in MATLAB for three representative values of the conversion rate: $g = 0.0067878$ (below the bifurcation threshold), $g = 0.5$ (moderate), and $g = 0.9$ (high). The initial conditions are set to $(50,50,50)$. The trajectories for the egg (x), hatchling (y), and predator (z) populations are shown in Figure 4.

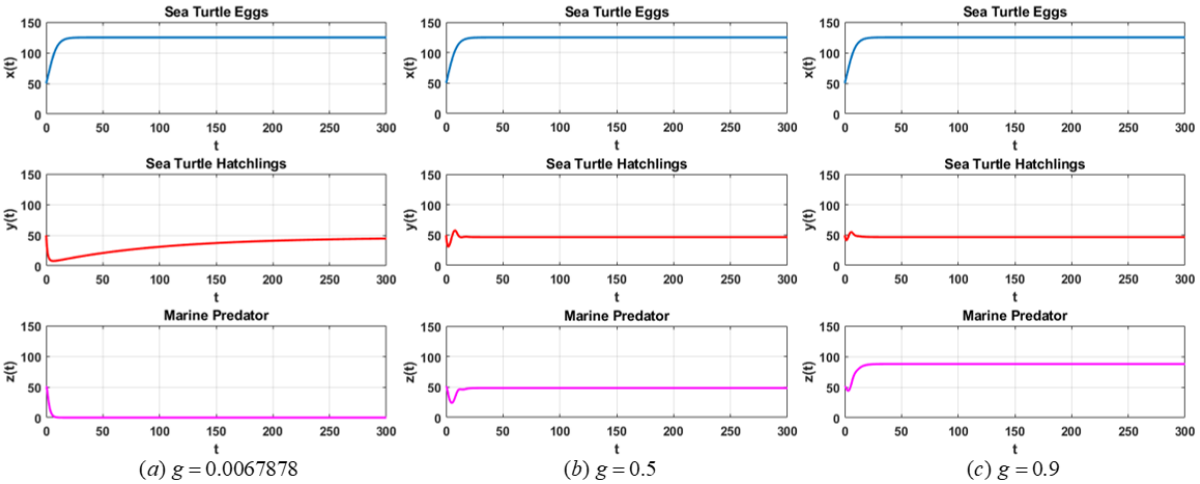

(*a*) $g = 0.0067878$ (*b*) $g = 0.5$ (*c*) $g = 0.9$

Figure 4: Time series of the sea turtle eggs (x), hatchlings (y), and marine predators (z) at three different conversion rates: $g = 0.0067878$ (predator extinction), $g = 0.5$ (coexistence), and $g = 0.9$ (high predator density)

For lower conversion rate $g = 0.0067878$ (Figure 4(a)), the egg population grows and stabilises around 125, while the hatchling population converges near 46. The predator population, however, declines rapidly to extinction. This outcome illustrates the first scenario, in which hatching success is too low to sustain predator populations. Although prey populations persist, the ecological balance is disrupted as predators are lost from the system.

For moderate conversion rate $g = 0.5$ (Figure 4(b)), all three populations remain present in the long term. The egg population again stabilises around 125, while both hatchlings and predators reach positive steady states. In contrast with the lower conversion case, this outcome shows a more balanced form of coexistence, where prey numbers are sufficient to support predators without causing excessive pressure on hatchlings. This type of behaviour reflects a stable and ecologically favourable state for the marine system.

For high conversion rate $g = 0.9$ (Figure 4(c)), the egg population still stabilises near 125. But the predator population grows substantially close to 90. The hatchling population, on the other hand, converges at a lower value of 45. Relative to the moderate scenario, these results show that higher conversion rates supply more food for predators, allowing them to grow. Although predators continue to persist under these conditions, the prey population becomes more vulnerable.

Overall, these time series simulations support the bifurcation and phase-plane analyses by showing how population levels evolve over time under different values of conversion rates. The results confirm that small variations in hatching success can shift among predator extinction, coexistence, and predator dominance simply by changing the conversion rate. From a management standpoint, the findings emphasise that sea turtle populations are highly sensitive to changes in hatching success. Conservation actions may therefore benefit from maintaining conversion rates that allow coexistence, rather than aiming only to maximise the number of hatchlings entering the sea.

4 Conclusions

This study examined a stage-structured prey-predator model to explore the dynamical interactions between sea turtles and marine predators when the conversion of eggs to hatchlings is varied. Through bifurcation analysis, the system undergoes a transcritical bifurcation in which stability shifts between unstable to stable states. Moreover, the phase-plane diagrams and time-series plots illustrate this outcome clearly: when hatching success is very low, predators die out; when hatching success reaches moderate levels, all populations can coexist; and when hatching success becomes too high, predator numbers grow, increasing predation pressure on hatchlings.

The main contribution of this study is the identification of the conversion rate g as a key bifurcation parameter that shapes the long-term behaviour of the system. While the earlier study by Khairuddin et al. [10] provided important insights into equilibrium dynamics of sea turtles and their predators, but it did not explore how small variations in parameters could lead to qualitative changes in stability. Thus, the present study extends this foundation by demonstrating, both theoretically and numerically, how the conversion rate acts as a driver of stability switching, and by visualising the exchange of stability at the transcritical bifurcation point. As compared with the findings of [10], which primarily emphasised equilibrium outcomes, this study contributes an additional layer of analysis that links bifurcation theory to ecological interpretation. In particular, it shows that predator persistence critically depends on hatching success, and that coexistence is only possible within a specific range of the conversion rate. This complementary perspective provides more detailed guidance for conservation efforts, suggesting that management should focus not only on increasing hatchling numbers but also on sustaining ecological balance between prey and predators.

Although the study provides new understanding of prey–predator dynamics, several avenues remain for further research. First, incorporating environmental variability, such as seasonal nesting cycles or stochastic fluctuations in hatching success, could capture more realistic ecological scenarios. Second, extending the model to include spatial dispersal of sea turtles and predators may reveal additional mechanisms of stability or coexistence. Finally, coupling the model with empirical field data would strengthen its predictive power and enhance its applicability to conservation strategies.

Acknowledgements

The author would like to thank the editor and reviewers for their thorough reading of the original manuscript and their numerous helpful comments and recommendations, which substantially enhanced the presentation of this work.

Conflict of Interest Statement

The authors agree that this research was conducted in the absence of any self-benefits, commercial or financial conflicts and declare the absence of conflicting interests with the funders.

Author Contributions

Zati Iwani Abdul Manaf contributed to the conception and design of the study, performed the data analysis and interpretation, and revised the manuscript. Muhammad Arif Azhar Khairulriza, Muhammad Syauqi Abdul Ghani, and Nur Syasya Iwanie Mohd Arifin drafted the initial version of the manuscript, contributed to the data analysis, and interpreted the results.

References

[1] K. V. H. Prasad, "Community Structure," in *Insect Ecology: Concepts to Management*, Singapore: Springer Nature Singapore, 2022, pp. 125–161. doi: 10.1007/978-981-19-1782-0_11.

[2] M. P. Bonsall, Michael B and Hassell, *Predator-prey interactions*. Oxford University Press Oxford, 2007.

[3] Jennifer Vonk and Todd K. Shackelford, Eds., "Character," in *Encyclopedia of Animal Cognition and Behavior*, Cham: Springer International Publishing, 2022, pp. 1292–1292. doi: 10.1007/978-3-319-55065-7_300363.

[4] M. Q. R. Pembury Smith and G. D. Ruxton, "Camouflage in predators," *Biological Reviews*, vol. 95, no. 5, pp. 1325–1340, Oct. 2020, doi: 10.1111/brv.12612.

[5] M. J. Sheriff, S. D. Peacor, D. Hawlena, and M. Thaker, "Non-consumptive predator effects on prey population size: A dearth of evidence," *Journal of Animal Ecology*, vol. 89, no. 6, pp. 1302–1316, Jun. 2020, doi: 10.1111/1365-2656.13213.

[6] B. T. Martin, M. A. Gil, A. K. Fahimipour, and A. M. Hein, "Informational constraints on predator–prey interactions," *Oikos*, vol. 2022, no. 10, Oct. 2022, doi: 10.1111/oik.08143.

[7] U. Jain, F. ul H. Nagrami, B. Sharma, Parul, and U. Sharma, "Definition, Scope, Characteristics, and Importance of Ecosystems," in *Epidemiology and Environmental Hygiene in Veterinary Public Health*, Wiley, 2025, pp. 365–384. doi: 10.1002/9781394208180.ch32.

[8] A. Mitra and S. Zaman, "Basics of Ecosystem," in *Environmental Science - A Ground Zero Observation on the Indian Subcontinent*, Cham: Springer International Publishing, 2020, pp. 87–116. doi: 10.1007/978-3-030-49131-4_4.

[9] R. Van De Walle, G. Logghe, N. Haas, F. Massol, M. L. Vandegehuchte, and D. Bonte, "Arthropod food webs predicted from body size ratios are improved by incorporating prey defensive properties," *Journal of Animal Ecology*, vol. 92, no. 4, pp. 913–924, Apr. 2023, doi: 10.1111/1365-2656.13905.

[10] M. A. A. Khairuddin, U. A. Mohd Roslan, H. Mohd Safuan, and M. U. Rusli, "Mathematical Model of the Population Dynamics of Sea Turtles at Chagar Hutang Beach, Malaysia," *J Sustain Sci Manag*, vol. 16, no. 4, pp. 327–336, Jun. 2021, doi: 10.46754/jssm.2021.06.024.

[11] Anis Syafinas Dahri, Ummu Atiqah Mohd Roslan, Harfiandri Damanhuri, and Mohd Uzair Rusli, "Estimating the Population Growth Curve of Sea Turtle Eggs Production in Terengganu, Malaysia: Mathematical Modelling Approach," *Journal of Advanced Research in Applied Sciences and Engineering Technology*, vol. 32, no. 1, pp. 332–342, Aug. 2023, doi: 10.37934/araset.32.1.332342.

[12] N. F. Lohmann, Kenneth J and Lohmann, Catherine MF and Brothers, J Roger and Putman, *Natal homing and imprinting in sea turtles*, vol. 3. CRC Press Boca Raton, FL, 2013.

[13] K. J. Lohmann and C. M. F. Lohmann, “There and back again: natal homing by magnetic navigation in sea turtles and salmon,” *Journal of Experimental Biology*, vol. 222, no. Suppl_1, Feb. 2019, doi: 10.1242/jeb.184077.
[14] L. L. Costa *et al.*, “Do costal erosion and urban development threat loggerhead sea turtle nesting? Implications for sandy beach management,” *Front Mar Sci*, vol. 10, Oct. 2023, doi: 10.3389/fmars.2023.1242903.
[15] M. R. Heithaus, *10 predators, prey, and the ecological roles of sea turtles*. CRC press, 2013.
[16] M. Mohd Roslan, UA and Jailani, MSO and Rusli, “Stability analysis for the dynamics of new sea turtle-human interaction model,” *Journal of Advanced Research in Dynamical and Control Systems*, vol. 11, no. 12, pp. 171–177, 2019.
[17] M. A. A. Khairuddin, U. A. M. Roslan, M. H. Mohd, and M. U. Rusli, “Sea turtle nest conservation-exploitation prey-predator model: Case study of Terengganu,” 2021, p. 040001. doi: 10.1063/5.0053370.
[18] M. T. Mohd Lutfi, U. A. Mohd Roslan, F. H. Ghane, and A. F. Embong, “Characterization of Basin of Attraction for An Attractor in A Discrete Prey-Predator Sea Turtle-Human Interaction Model using Stability Index Approach,” *Malaysian Journal of Fundamental and Applied Sciences*, vol. 18, no. 4, pp. 511–520, Oct. 2022, doi: 10.11113/mjfas.v18n4.2622.
[19] B. Dubey and A. Kumar, “Dynamics of prey–predator model with stage structure in prey including maturation and gestation delays,” *Nonlinear Dyn*, vol. 96, no. 4, pp. 2653–2679, Jun. 2019, doi: 10.1007/s11071-019-04951-5.
[20] C. Herrera, C. R. Duque, and H. Leiva, “Qualitative analysis of a mathematical model about population of green turtles on the Galapagos island,” *BIOMATH*, vol. 10, no. 2, Oct. 2021, doi: 10.11145/j.biomath.2021.07.293.
[21] M. Aguilera, M. Medina-Suárez, J. Pinós, A. Liria-Loza, and L. Benejam, “Marine debris as a barrier: Assessing the impacts on sea turtle hatchlings on their way to the ocean,” *Mar Pollut Bull*, vol. 137, pp. 481–487, Dec. 2018, doi: 10.1016/j.marpolbul.2018.10.054.
[22] U. A. Mohd Roslan and F. N. Harun, “Modeling the Impact of Pollution on Sea Turtles,” *Malaysian Journal of Fundamental and Applied Sciences*, vol. 19, no. 4, pp. 607–615, Aug. 2023, doi: 10.11113/mjfas.v19n4.2913.
[23] U. A. M. Roslan, F. N. Harun, and A. Azwani, “Dynamic Modelling for Assessing the Impact of Marine Debris on the Population of Sea Turtles,” *Journal of Quality Measurement and Analysis*, vol. 20, no. 2, Jul. 2024, doi: 10.17576/jqma.2002.2024.01.
[24] E. S. Siaw, S. Sathasivam, S. A. Adebayo, M. K. M. Ali, and V. Govindan, “Mathematical Approach for Conservation Initiatives to Model Population Dynamics of Endangered Sea Turtles in Chagar Hutang, Malaysia,” *Semarak International Journal of Animal Sciences and Zoology*, vol. 2, no. 1, pp. 1–6, 2025.
[25] M. Bodson, “Explaining the Routh–Hurwitz criterion: A tutorial presentation [Focus on Education],” *IEEE Control Systems Magazine*, vol. 40, no. 1, pp. 45–51, 2020.
[26] O. J. Omaiye and M. H. Mohd, “Computational Dynamical Systems Using XPPAUT,” in *Dynamical Systems, Bifurcation Analysis and Applications. DySBA 2018. Proceedings in Mathematics & Statistics, vol 295*, M. Mohd, N. Abdul Rahman, N. Abd Hamid, M. Yatim, and Y, Eds., Singapore: Springer, 2019.
[27] B. Ermentrout, *Animating Dynamical Systems: A Guide to XPPAUT for Researchers and Students*. Philadelphia: SIAM, 2002.
[28] K. A. Bouchard, Sarah S and Bjorndal, “Sea turtles as biological transporters of nutrients and energy from marine to terrestrial ecosystems,” *Ecology*, vol. 81, no. 8, pp. 2305–2313, 2000.
[29] E. Gyuris, “The rate of predation by fishes on hatchlings of the green turtle (Chelonia mydas),” *Coral Reefs*, vol. 13, no. 3, pp. 137–144, Jul. 1994, doi: 10.1007/BF00301189.
[30] Y. A. Kuznetsov, “Numerical Analysis of Bifurcations,” 2004, pp. 505–585. doi: 10.1007/978-1-4757-3978-7_10.